*Наносистеми, наноматеріали, нанотехнології*
*Nanosistemi, Nanomateriali, Nanotehnologii*
2022, т. 20, № 2, сс. 549–567



PACS numbers: 78.67.Bf, 81.07.Pr, 81.70.Pg, 87.14.ej, 87.19.xj, 87.64.Cc, 87.85.Rs

# Therapeutic Approach of Watermelon (*Citrullus lanatus*) Rind: Biosynthesis and Characterization of Selenium Nanoparticles

Namrata Jha[1], Sonia Johri[1], Sadhana Shrivastava[2], Poonam Gupta[1], and Kamini Yadav[2]

[1]*ITM University,*
*Jhansi Rd, Turari,*
*474001 Gwalior, Madhya Pradesh, India*
[2]*Jiwaji University*
*Sachin Tendulkar Rd, Kailash Nagar, Mahalgaon,*
*474001 Gwalior, Madhya Pradesh, India*

Watermelon (*Citrullus lanatus*) is a cheap and easily available fruit in the local markets of India. The rind, which is the outer layer of watermelon, is completely edible. It is the only fruit with 90% of water and is fully edible including its rind and seeds as they contain different types of nutrients, which are needed by human body in day-to-day life. The benefits in human body include reduced blood pressure, presence of different types of vitamins (such as vitamin A, B and C) as well as different types of minerals required by human body. The present study aims in evaluating the presence of different secondary metabolites in the watermelon rind. The therapeutic efficacy of watermelon rind against acrylamide toxicity in the lymphocyte cell line is studied. As selenium is an important micronutrient, an attempt has been made to prepare the selenium nanoparticles followed by its characterization.

Кавун (*Citrullus lanatus*) — дешевий і легкодоступний фрукт на місцевих ринках Індії. Шкірка, яка є зовнішнім шаром кавуна, повністю їстівна. Це єдиний фрукт з 90% води та повністю їстівний, включаючи шкірку та насіння, оскільки вони містять різні типи поживних речовин, які потрібні людському організму в повсякденному житті. Користь в організмі людини включає понижений артеріяльний тиск, наявність різних видів вітамінів (таких як вітамін A, B і C), а також різних видів мінералів, необхідних людському організму. Це дослідження спрямоване на оцінку наявности різних вторинних метаболітів у кавуновій шкірці. Вивчено терапевтичну ефективність шкірки кавуна проти токсичности акриламіду в клітинній лінії лімфоцитів. Оскільки селен є важливим мікроелементом, було зроблено спробу приготувати наночастинки селену з подальшою його характеризацією.

**Key words:** selenium nanoparticles, UV and visible radiations, FTIR, DSC, PSA.

**Ключові слова:** наночастинки селену, УФ- і видиме випромінення, інфрачервона спектроскопія на основі Фур'є-перетвору, диференційна сканувальна калориметрія, ґранулометрична аналіза.

*(Received 6 August, 2021 )*

## 1. INTRODUCTION

Emergences of efficient green chemistry methods for synthesis of nanoparticles from plant sources are an emerging field of research. Plants seem to be the best candidates for nanoparticle production as they are more stable and easily available. Moreover, the nanoparticles are more various in shape and size in comparison with those produced by other organisms. The advantages of using plant and plant-derived materials for biosynthesis have been explored widely all over the world for different experimental methods to extract out something beneficial ones [1]. The antioxidants, which were found in vegetables, are vitamin C, and E, carotenoids, and phenolic compounds, especially flavonoids. In the present era, there is increased attention towards the diet of humans in details, and their studies have been shown that a high intake of plant products is associated with the reduced risk of harmful diseases, which includes cancer as well [2]. Bio-nanotechnology is an eco-friendly and nontoxic perspective for the value of biomaterials along with the nanoparticles [3].

Watermelon (*Citrullus lanatus*) is a widely acceptable, edible fruit. Red part is sweet and edible, but the outer part is usually discarded and considered as of no use [4]. Watermelon is rich in carotenoids, some of which include lycopene, phytofluene, phytoene, beta-carotene, and lutein. Watermelon rind (WR) consists of different types of protein, functional group such as hydroxyl, carboxylic acid, pectin, citrulline, cellulose [4, 5].

An average watermelon contains about 30% of rind, 68% of flesh or pulp, and 2% of seeds. The rind is usually discarded, and it may be applied to feeds or used as fertilizer; but it is also edible and may be used as a vegetable. The rind has been shown to contain alkaloids, saponin, cardiac glycosides, flavonoids, phenol, moisture, lipid, protein, fibre, and carbohydrates. Earlier watermelon rind has been used as the biosorbent for the removal of dyes and heavy earth metals from the sample solution [6].

### 1.2. Acrylamide

There is high production of chemicals, which were having adverse

effect in the different products, which are made in the industries [7]. According to World Health Organization (WHO), more than 100 000 compounds are discharged in the society every year from different industries. The exposures of chemicals are also found in foods and different food products such as polycyclic aromatic hydrocarbons, aromatic amines, aminodyes, alkenes, which may also cause cancer [8].

Acrylamide has low molecular weight, is composed of carbon, hydrogen, nitrogen and oxygen atoms and can be soluble in water [9]. It is used in different industries in the form of polyacrylamide that was utilized as flocculent for the wastewater treatment, utilized as adhesives, soil stabilizers, in laboratory gels, by product of temperature-processed foods [10]. Acrylamide is considered as environmental and occupational pollutants. It can be formed during the Millard reaction, especially during the processing of food containing asparagine and glucose. Processed potato products, bread, breakfast cereals, biscuits, cookies, snacks, and coffee have been found to contain different levels of acrylamide residues [11].

### 1.3. Selenium Nanoparticles

The interest in nanoparticles has evolved due to their novel and enhanced capability as well as their applications in various areas such as places like chemistry, electronics, energy production area, drug production, computer products, *etc.* [12]. The emergence of nanoparticles has attracted a new approach towards the drug discovery and other related fields. Nanoparticles increase the therapeutic efficiency of ionized drugs, to improve the penetration of water-soluble compounds, proteins, peptides, vaccines, miRNAs, siRNA, DNA, and other biological components [13]. The biosynthesis of nanoparticles is more preferred through the green synthesis of nanoparticles, and the preparation of selenium nanoparticles (SeNPs) has been observed to have a wide range of applications biologically [13].

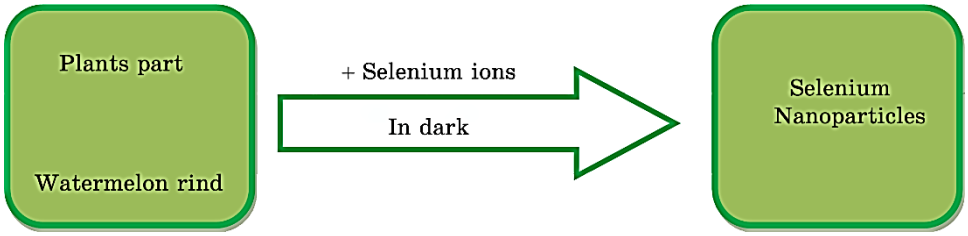


**Fig. 1.** Diagrammatic representation of formation of selenium nanoparticles.

Selenium nanoparticles have much high biological activity, which includes antihydroxyl radical property protective against the oxidation of DNA, as important elemental semiconductor, and improves activity of selenoenzyme, glutathione peroxidase prevention of free radical damage to cells and tissues *in vivo* [14].

Selenium is among those trace elements, which is required by the human body on a daily basis, which is approximately 40–300 mg as daily nutritional supplement for an adult [15]. An adult diet should contain at least 40 μg/day of Se to support the maximum expression of Se enzymes and, perhaps, as much as 300 μg/day to reduce the risk of cancer. Low Se can contribute to morbidity and mortality due to infectious as well as chronic diseases, and increasing Se intakes in all parts of the world can be expected to reduce cancer risks [15, 16].

The Recommended Dietary Allowance (RDA) for Se as per Food and Nutrition Board (USA) is of 55 μg/day (0.7 μmole/day) for adults [17]. SeNPs have potent free radicals' scavenging effects *in vitro* as well as *in vivo* conditions and protect DNA from oxidative damage. Several studies have reported that the SeNPs possess anticarcinogenic activity against several types of cancers, unique antimicrobial activities against *Candida albicans*, *Proteus mirabilis* and *Pseudomonas aeruginosa* [17].

Hence, the present study aims to study the secondary metabolites, toxicity of acrylamide in lymphocyte cell lines, to analyse the different functional groups, formation of selenium nanoparticles, and to characterize the selenium nanoparticles.

## 2. MATERIALS AND METHODS

### 2.1. Extract Preparation

The fresh fruits of watermelon were purchased from the local vendor. The watermelon was separated out, and watermelon rinds were washed thoroughly and chopped into pieces and dried for days under shadow (to remove moisture), then weighed and kept in oven at 85°C for 48 hours. A fine powder was obtained with the help of mortar pestle, which is then sieved and stored in desiccator for further use [16].

### 2.2. Aqueous Extract Preparation

#### *2.2.1. Decoction*

The fine powder of watermelon rind (1 g) was extracted by boiling

with distilled water (1:20) for around 4–6 hours, then filtered, and the extraction is repeated until the extract is colourless than the filtrate is concentrated then evaporated in water bath for further use [17]; 1 g was dissolved in 20 ml of water and the aqueous extract is used for further analysis.

## 2.3. Biosynthesis of Selenium Nanoparticles

2 ml of aqueous extract was added to 10 ml of 10 mM of sodium selenite solution, which is then kept in magnetic stirrer condition. Then, the solution was allowed for reduction in dark at $27 \pm 2°C$ in orbital shaker for 24 hours; then, the colour change is observed [16].

### *2.3.1. Chemical Profile of Watermelon Rind Extract*

Plants and its sources contain a wide range of secondary metabolites, and these ones were considered as potential reducing substances for biogenic production of nanoparticles. The total phenolic, flavonoids and tannin contents of watermelon rind extract were determined in order to evaluate its suitability in biogenic production of nanoparticles [16].

## 2.4. Phytochemical Screening of Watermelon Rind Extract [18, 19]

### *2.4.1. Test for Alkaloids (Mayer's Test)*

1 mg of rind extract was dissolved, followed by a few drops of acetic acid, followed by Mayer's reagent. Production of white precipitate indicates the presence of alkaloids.

### *2.4.2. Test for Carbohydrate (Fehling's Test)*

1 mg of rind extract was added to 1 ml of alcoholic solution followed by 1 ml of Fehling. Formation of red precipitate indicates the presence of carbohydrate.

### *2.4.3. Test for Steroids (Liebermann's Test)*

20 mg of rind extract was dissolved, followed by 1 ml of chloroform, 1 ml of acetic acid, and 1 ml of anhydride acetate. The solution is heated for 2–3 minutes that results in the conversion of pink colour solution to green colour solution, thereby indicating the presence of steroids.

### *2.4.4. Test for Saponins (FOAM Test)*

1 mg of rind extract was diluted in 7–8 ml of distilled water that results in the stable foam development and the presence of saponins.

### *2.4.5. Test for Tannins (Ferric Chloride Test)*

1 mg of rind extract was diluted in 1 ml of distilled water. Then, added 1 ml of 5% ferric chloride solution, the dark green or deep blue colour solution is obtained; this one results in the presence of tannins. Watermelon rind extract shows no colour change that indicates the absence of tannins.

### *2.4.6. Test for Phenols (Ferric Chloride Test)*

1 mg of rind extract was diluted in 1 ml of distilled water in a test tube. Then, added 1 ml of 5% ferric chloride solution, the blue or bluish black colour is obtained; this one results in the presence of phenols. Watermelon rind extract shows no colour change that indicates the absence of phenols in the solution.

### *2.4.7. Test for Coumarins (Sodium Hydroxide Test)*

2–4 mg of rind extract was taken in a test tube, and 1 ml of ethanol followed by 1 ml of 2N sodium hydroxide solution was added that results in the formation of dark fluorescence.

### *2.4.8. Test for Carboxylic Acid (Effervescence Test)*

20 mg of rind extract was diluted in 1 ml of distilled water in a test tube. Then, added 1 ml of sodium bicarbonate solution, dark bubble was obtained.

### *2.4.9. Test for Resin (Acetone Test)*

20 mg of rind extract was diluted in 1 ml distilled water and, added 1 ml of acetone solution, the solution becomes turbid; this one results in the presence of resin. Watermelon rind extract shows the turbidity in the obtained solution that indicates the presence of resin.

### *2.4.10. Test for Quinone (Sulphuric Acid Test)*

20 mg of rind extract was taken in a test tube and, added 1 ml of

100% ethanol and 1 ml of 2N sulphuric acid, this one results in the formation of pink/purple/red colour of the solution that results in the presence of quinone.

## 3. CHARACTERIZATION

### 3.1. UV–Vis Spectroscopy

The prepared selenium nanoparticles were characterized in a PerkinElmer UV–vis spectrophotometer to know the behaviour of SeNPs. The scanning range of the sample ranges from 200–1000 nm at a speed of 480 nm/min. The data taken by the UV–vis spectrophotometer is recorded and analysed by UV Winlab software. This one will help us to determine the analyte concentration or the chemical changes of a component in a solution. This instrument uses as a light source usually a deuterium or tungsten lamp, a sample holder and a detector. When the sample absorbs the light, it undergoes different changes such as excitation or deexcitation in the sample that results in the production of a range of spectrum [1].

### 3.2. FTIR (Fourier Transform Infrared) Spectroscopy

Fourier transform infrared spectroscopy is used to determine different functional group present in the solution of the watermelon rind extract, in the solution of selenium nanoparticles. The rind extract was dried and grounded with mortar pestle, and spectrum was taken at the wavelength of 4000–400 $cm^{-1}$. The SeNPs solution was dried and grounded in mortar pestle for the preparation of fine powder. Then, Fourier transform infrared spectrum of selenium nanoparticles was taken from 4000 to 400 $cm^{-1}$ wavelength in the FTIR machine [16].

### 3.3. PSA (Particle Size Analyser)

The particle sizes were analysed with the instrument for the particle size analysis, Shimadzu SALD-2300; the measurement was taken, and refractive index of the medium was taken at 1.07 (water) [20].

### 3.4. DSC (Differential Scanning Calorimetry)

The thermal analysis was conducted with the instrument for the differential scanning calorimetry, TGA-50, SHIMADZU Thermogravimetric Analyser, and the instrument was calibrated with the

sample from 15°C to 300°C [21].

## 4. *In vitro* STUDY

### 4.1. Chemical and Reagent

Acrylamide, Roswell Park Memorial Institute (RPMI) 1640 Medium were procured from Sigma Aldrich, ficoll plaques, EDTA, fetal bovine serum (FBS), $NaHCO_3$, streptomycin, gentamycin, penicillin G, KCl, NaCl, $KH_2PO_4$, triple distilled water, trypan blue dye, MTT assay, acetic acid, TCA, tris base.

### 4.2. Treatment and Dose Preparation

A suspension of (5 mM) acrylamide (AA) was prepared in triple distilled water.

### 4.3. *In vitro* Therapeutic Efficacy

Evaluation of therapeutic effectiveness of aqueous extract of watermelon rind against acrylamide induced cytotoxicity on isolated lymphocyte was carried out (see also *5.6.1*).

### 4.4. Watermelon Rind Aqueous Extract

Watermelon rind aqueous extract (15 mg) was dissolved in RPMI medium and volume made up to 3 ml. A different dose of WR aqueous extract was administered to the 96 well plates to select the optimum dose of aqueous extract.

### 4.5. *In vitro* Experimental Design

Preparation of 0.82 g RPMI medium, 100 mg $NaHCO_3$, 20 mg streptomycin, 37.5 ul gentamycin, 6 mg penicillin G was dissolved in 20 ml autoclaved triple distilled water, and 10 ml fetal bovine serum (FBS) was added to it.

### 4.6. Isolation of Lymphocyte

A blood sample was derived from a healthy female rat and collected with the help of capillary in a test tube with one pinch of EDTA. 2 ml of phosphate buffer saline (PBS) pH 7.4 used for the dilution air was layered on 4 ml Ficoll-Paque and centrifuged for 10 min at 2000 rpm.

The white buffy layer containing lymphocytes was separated and transferred to a new tube. Collected lymphocyte layer was diluted with PBS pH 7.5 in the ratio of 1:1 and centrifuged at 2000 rpm for 10 min, and the pellet was collected. After washing cell with RPMI 1640 (containing 10% FBS) twice, cell was cultured using RPMI 1640 (containing 10% FBS) and 1% antibiotic in the flask and incubated in $CO_2$ incubator containing 5% $CO_2$ at the temperature of 37°C [22].

### 4.7. Maintenance

Lymphocytes cells were grown in tissue culture flask with complete growth medium at 37°C in an atmosphere of 5% $CO_2$ and 90% relative humidity in $CO_2$ incubator. The medium was changed as the colour changes.

The fresh medium was placed in culture flask 5–7 under sterile condition. Passaging was done at the subconfluent stage of cells, which is depending on the mass-doubling time of cell.

### 4.8. Subculturing

The exhausted medium was changed by the fresh medium as per requirement. The medium of the flask having subconfluent growth was changed followed by centrifugation at 2000 rpm for 10 min. After centrifugation, pallet was collected. This one is then washed with phosphate buffer saline. The tube was centrifuged at 2000 rpm at 10 min; supernatant was discarded. The cells were resuspended in the complete growth medium and were counted and checked for viability with trypan blue. After achieving 70–80% confluence, the next subculturing was performed [23].

### 4.9. Cell Viability Assay

Cell viability in the number of healthy cells in a sample determines the amount of cells (regardless of phase around the cell cycle), which are living or dead, based on a total cell sample.

### 4.10. Calculation

$$\% \text{ cell growth} = \frac{\text{cell growth in the presence of test material}}{\text{cell growth in the absence of test material}},$$

$$\% \text{ growth inhibition} = 100\% \text{ cell growth}.$$

## 5. RESULTS & DISCUSSION

### 5.1. Biogenic Synthesis and Characterization of SeNPs

It was noted that the extraction efficiency achieved by using boiling water was much effective and greater than that achieved with other methods using 80% methanol and shows the extraction efficiency much higher than that of the other alcoholic method [24].

Originally, sodium selenite solution was colourless. The colour of sodium selenite turned into brick red with the addition of watermelon rind extract after 24 hours (Fig. 2). The formation of brick-red solution was due to the excitation of the surface-plasmon resonance, and it was an indication for reduction of sodium selenite into elemental selenium. The reduction of sodium selenite into SeNPs can occur by the action of phenolics, flavonoids, and tannins of wa-

*a* *b*

**Fig. 2.** These figures show the starting of the incubation of extract (*a*) or the changes in the colour after the completion of incubation period (*b*).

**TABLE 1.** Phytochemical screening of aqueous extract of watermelon rind.

| Test | Function | Result |
|---|---|---|
| Mayer's test | alkaloids | negative |
| Fehling's test | carbohydrate | positive |
| Liebermann's test | steroids | positive |
| Saponins test | foam | positive |
| Ferric chloride test | tannin | positive |
| Ferric chloride test | phenol | less amount |
| Sodium hydroxide test | coumarins | positive |
| Effervescence test | carboxylic | positive |
| Acetone test | resin | positive |
| Sulphuric acid test | quinone | positive |

termelon rind. Then, this is further confirmed by the UV–visible spectrophotometer [16].

### 5.2. Phytochemical Screening of Aqueous Extract of Watermelon Rind

The results of the phytochemical analysis of aqueous extract of watermelon rind showing the presence of different phytochemicals in less amount or in high amount in the extract. The presence of carbohydrate, steroids, saponins, tannins, coumarins, carboxylic acid, quinine, and rennin was in higher amount in the solution, whereas, there was also found less amount of phenol, and the absence of alkaloids was detected. The presence of secondary metabolites such as alkaloids, carbohydrates, steroids, saponins, coumarins, carboxylic acid, resin and quinone was determined using different tests that make the changes in the solution to reveal the presence of secondary metabolites. The phytochemicals' analysis provides us knowledge about the different bioactive elements, which were present in the solution; this one shows the presence of different primary and secondary metabolites in the extract.

### 5.3. UV–Vis Spectroscopy

Synthesis of selenium nanoparticles using sodium selenite has been reported by the UV–vis spectroscopy. To see the presence of the selenium nanoparticles present in the solution, UV–vis spectra of SeNPs were recorded, and the formation of selenium nanoparticles were visualized with the change in the colour of the solution. The spectra show that there is increase in the spectra as moving forward from 200 nm. The absorption maximum is shown after 203 nm that determines that the extract is reduced, and SeNPs has been stabilized at this wavelength. The graph of selenium nanoparticles has increased in the spectra from the range of 200–300 nm (Fig. 3) and shows the presence of selenium at the range from 220 nm to 385 nm in the aqueous extract of the watermelon rind. There was a high peak at 200 nm to 358 nm in Fig. 4 after the incubation period and the high peak at 203 nm to 288 nm in Fig. 5 before the incubation period. The UV data analysis supports the formation of selenium nanoparticles from the watermelon rind extract at 200–300 peak [16].

### 5.4. FTIR (Fourier Transform Infrared) Analysis

The Fourier transform infrared analysis of aqueous extract of watermelon rind shows the major absorption bands, which appear at 3340.03 $cm^{-1}$ and another at 1634.72 $cm^{-1}$, that is due to the pres-

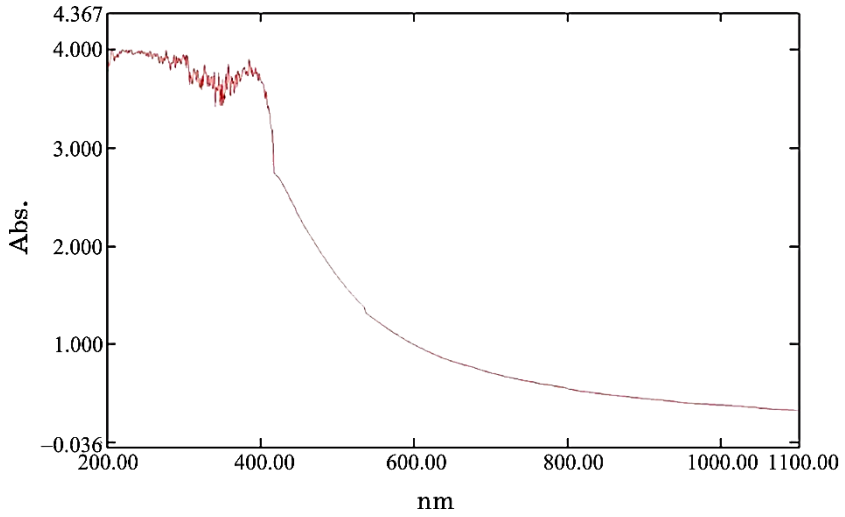


**Fig. 3.** UV–visible spectrum of the aqueous extract of watermelon rind.

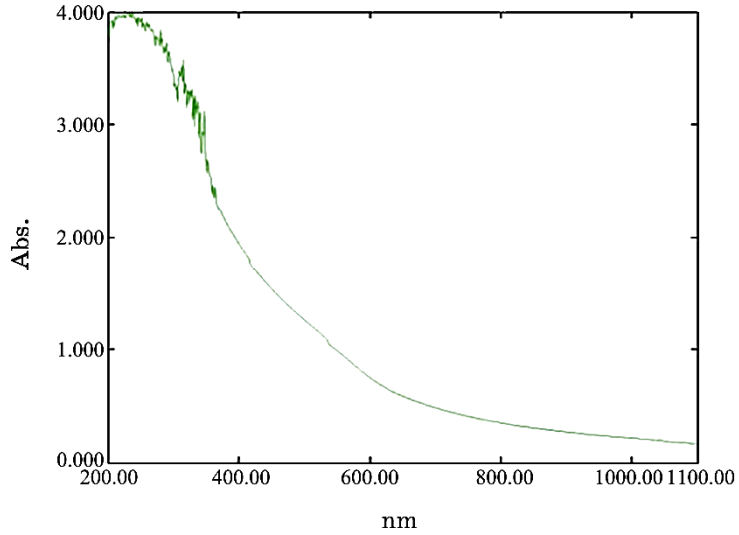


**Fig. 4.** UV–vis spectra for the presence of SeNPs after the incubation of the solution prepared.

ence of O–H stretching, which is in alcohol, and another is due to the C=C stretching, which is in alkene, shown in Table 2 and Fig. 6.

The Fourier transform infrared analysis of SeNPs of watermelon rind extract shows some major absorption bands, which are appeared at 3278.45, 2921, 2849, 1638, 1535, 1395, 1238, 1030, 539 $cm^{-1}$. The bands, which are appeared at different wavelength, have

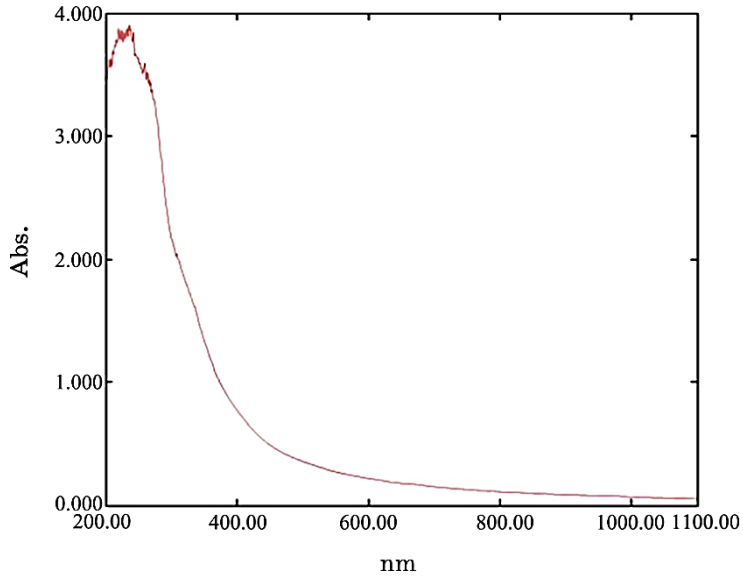


**Fig. 5.** UV–vis spectra before the solution kept in incubation.

**TABLE 2.** Functional groups of aqueous extract watermelon rind.

| No. | Absorbance, $cm^{-1}$ | Group | Compound | Appearance |
|---|---|---|---|---|
| 1 | 3340.03 | O–H stretch | alcohol | strong |
| 2 | 1634.72 | C=C stretch | alkene | medium |

different stretches at 3278.45 $cm^{-1}$ that is due to the presence of O–H stretching, which is of carboxylic acid. Another absorption peak at 2921 $cm^{-1}$ is due to the presence of C–H bond of methylene asymmetric. The band at 2849 $cm^{-1}$ is due to the presence of O–$CH_3$ bond of methoxy. The strong band at 1638 $cm^{-1}$ shows the presence of C=C, which is of alkene. Another band at 1535 $cm^{-1}$ shows the presence of >N–H, which is of secondary amine. The short band at 1395 $cm^{-1}$ shows the presence of O–H, which is of tertiary alcohol. The short band at 1238 $cm^{-1}$ is due to C–O stretching, which is of alkyl aryl ether. The strong band at 1030 $cm^{-1}$ is due to C–C stretching vibration and, at 539 $cm^{-1}$, it is due to OH bending of the phenolic group, as shown in Table 3.

Fourier transform infrared spectrum indicates that the variations in the graph show the presence of secondary metabolites, which are responsible for the reduction of the selenium ions and the formation of SeNPs due to their reduction and capping process. This implies that Fourier transform infrared results analysed show that the SeNPs were successfully synthesized using the watermelon rind ex-

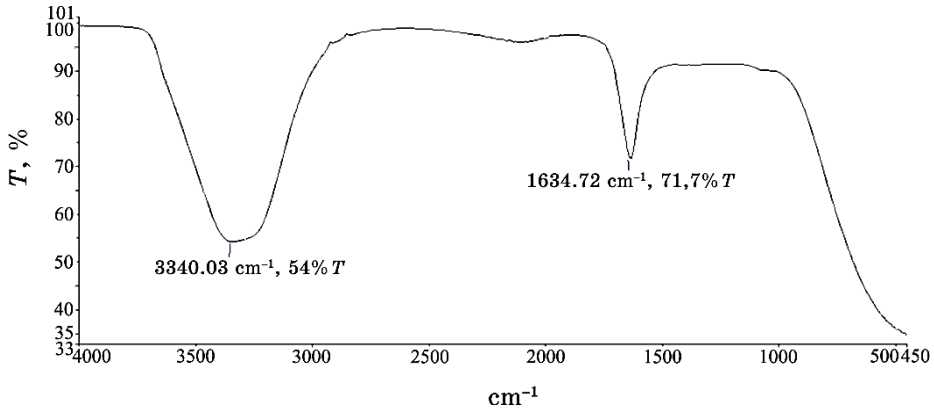


**Fig. 6.** Fourier transform infrared spectrum of aqueous extract of watermelon rind.

**TABLE 3.** Functional groups of selenium nanoparticles extracted from watermelon rind extract.

| No. | Absorption, $cm^{-1}$ | Group | Compound | Appearance |
|---|---|---|---|---|
| 1 | 3278.45cm | O–H stretching | alcohol | strong |
| 2 | 2921 cm | C–H stretching | methylene asymmetric | strong |
| 3 | 2849 cm | O–$CH_3$ stretching | methoxy | medium |
| 4 | 1638 cm | C=C stretching | alkene | strong |
| 5 | 1535 cm | >N–H stretching | secondary amine | medium |
| 6 | 1395 cm | O–H stretching | tertiary alcohol | medium |
| 7 | 1238 cm | C–O stretching | alkyl aryl ether | weak |
| 8 | 1030 cm | C–C stretching | | strong |
| 9 | 539 cm | OH stretching | phenolic | strong |

tract [20, 28] (Fig. 7).

### 5.5. PSA and DSC

The particle size analysis was carried out by particle size analyser obtained. In present study, the laser diffraction studies reveal that the particle size obtained from highly dispersed mixture was in two areas; on the scale of normalized particle amount in 0–10, the particle diameter was of 0.05–0.4 μm, and, in 0–5, the particle diameter found to be in range 48–100 μm [26, 27]. The image in Fig. 8 shows that the size of the nanoparticles is within the nanoscale.

The differential scanning calorimetry gives us the thermograph

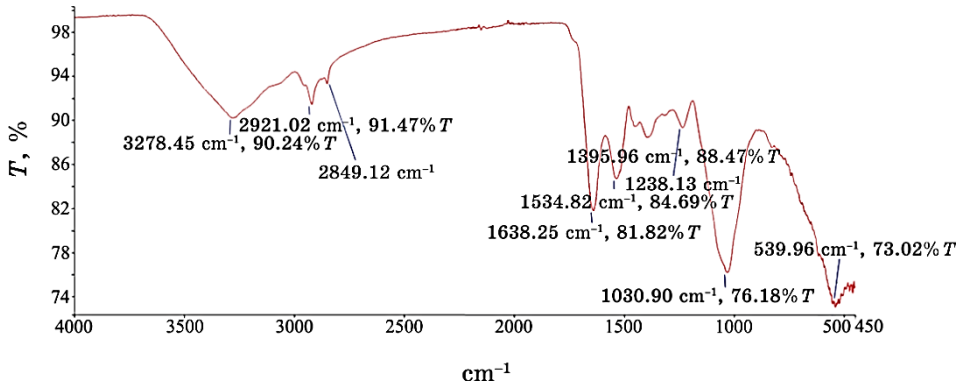


**Fig. 7.** Fourier transform infrared spectrum of selenium nanoparticles synthesized from watermelon rind extract.

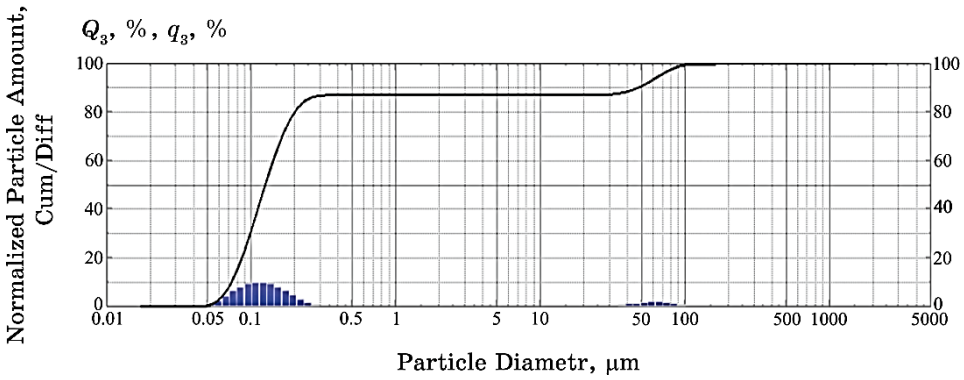


**Fig. 8.** Particle size analysis of selenium nanoparticles.

of the nanoparticles with multiple peaks, which determine the different crystalline features of the particles provided into the instrument. The particles were recorded at 50°C (the exothermic transition of the particles); at 300°C, the endothermic melting peaks were observed [28, 29]. The graph in Fig. 9 shows the nanocrystalline nature of the particles losing their capability at 353°C.

## 5.6. *In vitro* Studies

### *5.6.1. Evaluation of Therapeutic Effectiveness of Aqueous Extract of Watermelon Rind against Acrylamide Induced Cytotoxicity on Isolated Lymphocyte*

Cytotoxicity of acrylamide on isolated lymphocytes was measured on

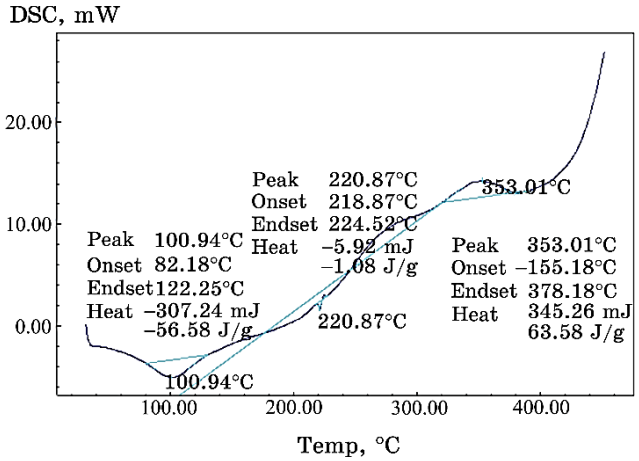


**Fig. 9.** Differential scanning calorimetry analysis of selenium nanoparticles.

isolated lymphocytes. The therapeutic effectiveness of aqueous extract of watermelon rind was evaluated after acrylamide exposure. Control group depicted 98% cell viability, while acrylamide-exposed group at 5 Mm concentration revealed that the cell viability was decreased potentially up to 24%. Treatment with aqueous extract of watermelon rind on acrylamide-exposed group showed the significant lymphocyte protective activity in concentration-dependent manner. Lymphocytes were treated with aqueous extract of watermelon rind at 6 different concentration ranges from 25–500 ug/ml after acrylamide exposure on lymphocytes. Treatment with aqueous extract of watermelon rind at a dose of 500 ug/ml concentration showed maximum cell viability as more than 90% than cell at lower concentration.

Different extracts of melon showed the iron and copper ions' chelating activity at different concentrations, especially aqueous extract of watermelon rind. The proliferation was inhibited by 20–85% at extract concentrations of 0.1–1.0 mg/ml in kidney carcinoma, cervical adenocarcinoma and cervical carcinoma. The results suggest that watermelon-residues' extracts display a high antioxidant activity *in vitro* assays and have effective biological activity against the growth of human tumour cells [30].

Based on *in vitro* studies, aqueous extract was more effective on lymphocyte. Extremely significant activity was observed in acrylamide exposure on lymphocyte, *i.e.*, $IC_{50} = 65.30$ μg/ml.

Aqueous extract of watermelon rind showed significant activity with lowered $IC_{50}$. IC values of aqueous extract of watermelon rind were calculated to compare the therapeutic potential of plant ex-

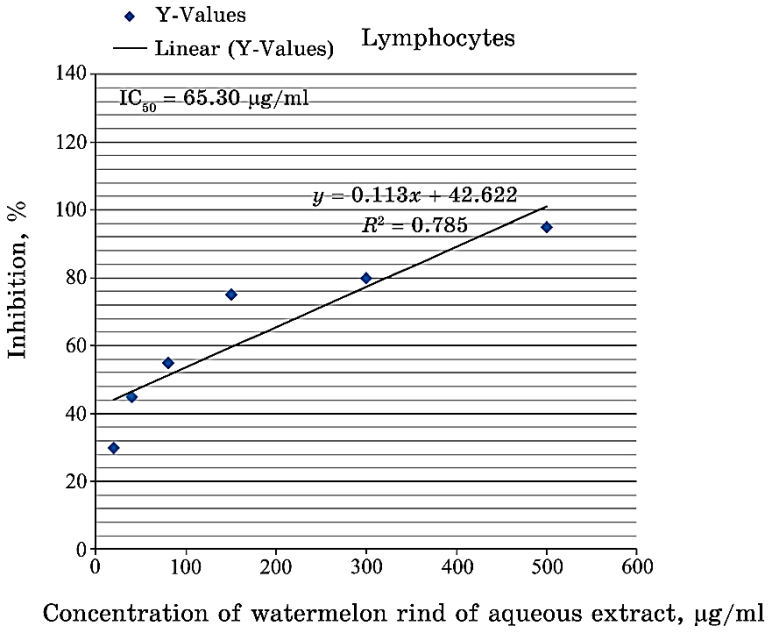


**Fig. 10.** $IC_{50}$ of aqueous extract of watermelon rind.

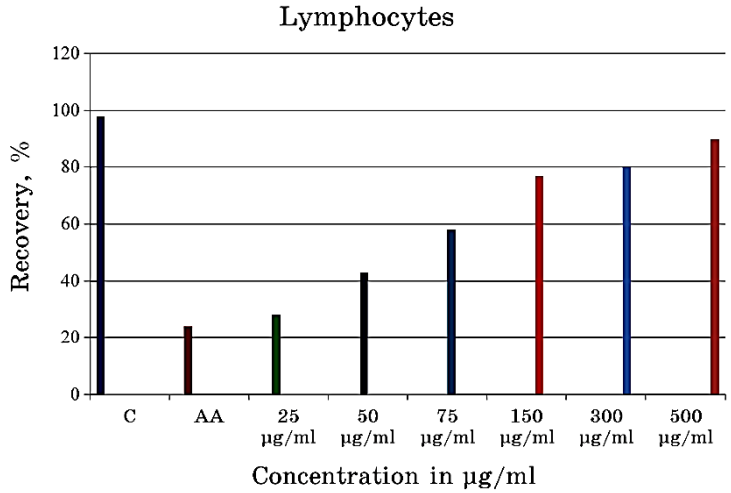


**Fig. 11.** Effect of aqueous extract of watermelon rind on acrylamide exposed lymphocytes.

tract against acrylamide (AA) induced cytotoxicity.

The lower $IC_{50}$ value corresponds to the maximum activity of treatment against particular cell [23, 30].

## 6. CONCLUSION

The present studies show that the biosynthesis of SeNPs by using watermelon (*Citrullus lanatus*) rind extracts is economically environmental friendly and nontoxic process. The characterization of the nanoparticles through UV–visible spectroscopy reveals the presence of selenium nanoparticles, which were responsible for the absorption of the light. FTIR analysis confirms the presence of different functional groups, which belong to biomolecules on the surface of the SeNPs. The DSA and PSC reveals size of the particle and the nature of the particles present in the solution of the nanoparticles, their nature at different temperatures that determines the nanosize of the particles. Determination of secondary metabolites, *in vitro* approach against acrylamide toxicity, characterization by UV–visible spectroscopy, FTIR, followed by the biosynthesis of SeNPs, promotes further research in field of medicine—nanodrugs.

## ACKNOWLEDGEMENT

The authors would like to acknowledge the support of the staff of the Central Instrumentation Facility, Jiwaji University, Gwalior, M.P. and ITM University, Gwalior, M.P. for providing instrumental facilities and analyses of data.

## REFERENCES

1. V. Alagesan and S. Venugopal, *Bio Nano Sci.*, **9**: 105 (2019); https://doi.org/10.1007/s12668-018-0566-8
2. C. Worarat and G. Wandee, *J. Sci. Technol.*, **31**, No. 4: 419 (2009).
3. M. Yazhiniprabha and B. Vaseeharan, *Mater. Sci. Eng. C: Mater. Biol. Appl.*, **103**: 109763 (2019); https://doi.org/10.1016/j.msec.2019.109763
4. R. Lakshmipathy, P. Reddy, B. Sarada et al., *Appl. Nanosci.*, **5**: 223 (2015); https://doi.org/10.1007/s13204-014-0309-2
5. J. K. Patra and K. H. Baek, *Int. J. Nanomed.*, **10**: 7253 (2015); https://doi.org/10.2147/IJN.S95483
6. M. Huang, J. Jiao, J. Wang, Z. Xia, and Y. Zhang, *Environ. Pollut.*, **234**: 656 (2018); https://doi.org/10.1016/j.envpol.2017.11.095
7. M. Kianfar, A. Nezami, S. Mehri, H. Hosseinzadeh, A. W. Hayes, and G. Karimi, *Drug & Chem. Tox.*, **43**, Iss. 6: 595 (2018); https://doi.org/10.1080/01480545.2018.1536140
8. M. Kopanska, R. Muchacka, J. Czecha, M. Batoryna, and G. Formicki, *J. Physiol. Pharmacol.*, **60**, No. 6: 847 (2018); https://doi.org/10.26402/jpp.2018.6.03
9. J. Kumar, S. Das, and S. L. Teoh, *Front. Nut.*, **5**: Article 14 (2018); https://doi.org/10.3389/fnut.2018.00014
10. E. Zamani, M. Shokrzadeh, and A. Ziar, S. Abedian-Kenari, and F. Shaki,

*Hum. Exp. Toxicol.*, **37**, No. 8: 859 (2018); https://doi.org/10.1177/0960327117741753
11. R. Kirupagaran, A. Saritha, and S. Bhuvaneswari, *J. NanoSci. Tech.*, **2**, No. 5: 224 (2016).
12. A. Khurana, S. Tekula, M. A. Saifi, P. Venkatesh, and C. Godugu, *Biomed. Pharmacother.*, **111**: 802 (2019); https://doi.org/10.1016/j.biopha.2018.12.146
13. G. Sharma, A. R. Sharma, R. Bhavesh, J. Park, B. Ganbold, J. S. Nam, and S. S. Lee, *Molecules*, **19**, No. 3: 2761 (2014); https://doi.org/10.3390/molecules19032761
14. W. Zhang, Z. Chen, H. Liu, L. Zhang, P. Gao, and D. Li, *Col. Surf. B: Biointerfaces*, **88**, No. 1: 196 (2011); https://doi.org/10.1016/j.colsurfb.2011.06.031
15. M. Navarro-Alarcon and C. Cabrera-Vique, *Sci. Total. Environ.*, **400**, Nos. 1–3: 115 (2008); https://doi.org/10.1016/j.scitotenv.2008.06.024
16. L. Gunti, R. S. Dass, and N. K. Kalagatur, *Front. Microbiol.*, **10**: 931 (2019); https://doi.org/10.3389/fmicb.2019.00931
17. K. Yamasaki, A. Hashimoto, Y. Kokusenya, T. Miyamoto, and T. Sato, *Chem. Pharm. Bull.*, **42**, No. 8: 1663 (1994); https://doi.org/10.1248/cpb.42.1663
18. R. S. Kumar, C. Venkateshwar, G. Samuel, and S. G. Rao, *Int. J. Eng. Sci. Invent.*, **2**, No. 8: 2319 (2013).
19. S. Ali, M. R. Khan, Irfanullah, M. Sajid, and Z. Zahra, *BMC Complement. Altern. Med.*, **18**: Article No. 43 (2018); https://doi.org/10.1186/s12906-018-2114-z
20. N. Srivastava and M. Mukhopadhyay, *J. Clust. Sci.*, **26**: 1473 (2015); https://doi.org/10.1007/s10876-014-0833-y
21. Q. Chu, W. Chen, R. Jia, X. Ye, Y. Li, Y. Liu, Y. Jiang, and X. Zheng, *J. Hazardous Mat.*, **393**: 122364 (2020); https://doi.org/10.1016/j.jhazmat.2020.122364
22. S. S. Ngema, A. K. Basson, and T. S. Maliehe, *Physics and Chemistry of the Earth, Parts A/B/C*, **115**: 102821 (2020); https://doi.org/10.1016/j.pce.2019.102821
23. R. Pascua-Maestro, E. González, C. Lillo, M. D. Ganfornina, J. M. Falcyn-Pérez, and D. Sanchez, *Front. Cell Neurosci.*, **12**: 526 (2019); https://doi.org/10.3389/fncel.2018.00526
24. H. B. Li, Y. Jiang, C. C. Wong, K. W. Cheng, and F. Chen, *Anal. Bioanal. Chem.*, **388**, No. 2: 483 (2007); https://doi.org/10.1007/s00216-007-1235-x
25. N. Srivastava and M. Mukhopadhyay, *Pow. Tech.*, **244**: 26 (2013); https://doi.org/10.1016/j.powtec.2013.03.050
26. F. Tateo and M. C. Bononi, *Ital. J. Food Sci.*, **15**: 149 (2003).
27. N. C. Bell, C. Minelli, and A. G. Shard, *Anal. Methods*, **5**: 4591 (2013); https://doi.org/10.1039/C3AY40771C
28. M. Kazemi, A. Akbari, H. Zarrinfar et al., *J. Inorg. Organomet. Polym.*, **30**: 3036 (2020); https://doi.org/10.1007/s10904-020-01462-4
29. S. D. Clas, C. R. Dalton, and B. C. Hancock, *Pharm. Sci. Technol. Today*, **2**, No. 8: 311 (1999); https://doi.org/10.1016/s1461-5347(99)00181-9
30. P. M. Rolim, G. P. Fidelis, C. E. A. Padilha, E. S. Santos, H. A. O. Rocha, and G. R. Macedo, *Braz. J. Med. Biol. Res.*, **51**, No. 4: 1414 (2018); https://doi.org/10.1590/1414-431x20176069